Thin Solid Films 519 (2010) 823–828

Contents lists available at ScienceDirect

Thin Solid Films

journal homepage: www.elsevier.com/locate/tsf

Surface deformation of amorphous silicon thin film on elastomeric substrate

Sangwook Lee [a], Jungmok Seo [a], Ja Hoon Koo [a], Kyeong-Ju Moon [b], Jae-Min Myoung [b], Taeyoon Lee [a,*]

[a] Nanobio Device Laboratory, School of Electrical and Electronic Engineering, Yonsei University, 134 Shinchon-Dong, Seodaemun-Gu, Seoul 120-749, South Korea
[b] Information and Electronic Materials Research Laboratory, Department of Materials Science and Engineering, Yonsei University, 134 Shinchon-Dong Seoul 120-749, South Korea

ARTICLE INFO

Article history:
Received 8 January 2010
Received in revised form 26 August 2010
Accepted 26 August 2010
Available online 28 September 2010

Keywords:
a-Si
Thin films
Buckling
Wrinkle patterns
Herringbone structure
Polydimethylsiloxane
Transfer printing
Textured structures

ABSTRACT

Stiff thin layers on compliant substrates can generate various surface structures using equi-biaxial stress caused by large thermal expansion rate differences. We investigated the detailed understanding on the evolution of self-assembled wrinkle patterns of ultra-thin amorphous silicon (a-Si) layers on poly-dimethylsiloxane substrate. It turns out that the generation of various wrinkle patterns depends on the position of their orientation, film thicknesses, mechanical properties of the a-Si films, and the amount of pre-strain. The various self-assembled patterns include one-dimensional wavy patterns, randomly ordered two-dimensional structured patterns, and herringbone structures. The self-assembled wrinkles can be characterized by the wavelength and amplitude of the distinct structures: the amplitudes of the various patterns increase as the amount of pre-strain increases, while the wavelengths remain constant within our experimental ranges. The experimental results of the wavelengths and amplitudes for the wavy structured patterns of 270-nm-thick a-Si layer are in good agreement with the theoretical solutions of the single crystalline silicon (c-Si) model, which implies that the theoretical modeling of the deformation of c-Si film can be expandable to the case of a-Si film deformations.

1. Introduction

Amorphous silicon (a-Si) thin films have been widely used in a large variety of applications such as thin film transistor [1,2], separation of macro-molecules [3], anodes in rechargeable batteries [4,5], image sensor [6], and photovoltaic devices [7], due to their low temperature process, capability for large-scale applications, and low cost in production. In recent reports, controllable techniques to modify structures and features on surface of a-Si thin films have received great attentions for increasing the surface-area-to-volume ratio, enhancing the performance of the device, and reducing the adhesion and friction forces, compared to the original flat surface [8–10]. However, the conventional techniques of modifying the surface structure generally require an incorporation of additional layers or particles on to the surface, which is highly redundant.

One simple method to organize deformed patterns, especially for buckled systems, is based on utilizing the reinstatement force in materials with contractibility [11]. In this technique, a metal thin film is directly deposited [12,13] or single crystal silicon (c-Si) ribbons are physically transferred [14] on top of a heated elastomer such as Polydimethylsiloxane (PDMS), followed by releasing the residual pre-strain in such substrates. Consequently, the films/ribbons experience a compressive stress due to a large thermal expansion discrepancy between the layer and the heated elastomer, which leads to the formation of spontaneous, complex and ordered structures on the transferred layers. It has been reported that the evolution of wrinkled patterns depends on several factors including the thickness of the film, mechanical properties of the material, and the amount of pre-strain [13]. Several researches were conducted on the method to controllably manipulate the deformation of various material-based thin films to desired dimensions and patterns by varying the aforementioned parameters [12,15–17]. Nevertheless, there have been little efforts to acquire the fundamental understanding on the buckling phenomena of a-Si thin film; only in our previous work [18] the fundamentals on the instability of a-Si film during the initial stages of its detachment from a-Si/SiO_2/Si system were revealed using a careful *in-situ* observation. In general, a-Si thin films are advantageous compared with c-Si films since it is much more convenient to obtain large-area a-Si thin films as the process for obtaining the detached a-Si thin membranes does not require creating holes or making nanoribbons to facilitate the etching of sacrificial oxide layers which is mandatory in the case of c-Si or III-V compound semiconductor films [14,17,19,20].

Here, we focused on the investigation of the structural instability of ultrathin a-Si layer under the equi-biaxial compressive stresses of the elastomer substrates to obtain thin layers with desired self-assembled textures. The full courses of the structural evolutions of the a-Si layer by applying the thermal strain were closely observed using an *in-situ* optical microscope: the layers on PDMS substrates were developed into various wavy geometries by equi-biaxial compressive stress. The various self-assembled wavy patterns including one or two-dimensional structures on a-Si thin films are quantitatively and analytically examined. For the 270-nm-thick a-Si layer, the measured

* Corresponding author. Tel.: +82 2 2123 5767; fax: +82 2 313 2879.
E-mail address: taeyoon.lee@yonsei.ac.kr (T. Lee).

0040-6090/$ – see front matter © 2010 Elsevier B.V. All rights reserved.
doi:10.1016/j.tsf.2010.08.140

geometric factors (wavelength and amplitude) of one-dimensional wrinkled and two-dimensional structured patterns are in accordance with the theoretical values estimated from the c-Si deformation model. These results indicate that the analytical solutions for the detachment of c-Si films can be expandable to the structural deformation of a-Si membranes.

2. Experimental procedure

The sacrificial layer of 300-nm-thick silicon dioxide (SiO_2) was initially deposited on to a c-Si substrate using dry furnace in O_2 ambient at 800 °C, followed by a deposition of hydrogenated a-Si film with thickness of 270 nm through plasma enhanced chemical vapor deposition system using gaseous mixtures of SiH_4, He, and H_2 at 280 °C.

Fig. 1(a) schematically illustrates the procedures for obtaining periodic one- or two-dimensional buckling of the a-Si membranes on PDMS. The a-Si:H/SiO_2/Si substrates were immersed in aqueous hydrofluoric acid (HF) with concentration of 49–51% to etch the sacrificial oxide layer and consequently detach the a-Si film. As the HF solution permeate through the a-Si layer, the oxide layer below the a-Si film is gradually etched and a-Si film is detached from the mother wafer, eventually becoming free after the etching process is finalized. Prior to transferring the fully detached a-Si film onto the PDMS, an elastomeric material, the PDMS was cured using a mixture of Sylgard 184 base and curing agent (of which the volume composition is 10:1) [21], at room temperature during 24 h. The fully detached a-Si film was then transferred onto the PDMS, which was pre-strained by heating on the hot plate with ranging the annealing temperature from 105 °C to 150 °C (the variation of the temperature is given to apply different amount of pre-strains) for sufficient amount time. The a-Si/PDMS sample rests on the hot plate for few more minutes to create an adhesive bonding between the a-Si film and the PDMS [14]. After that, the a-Si/PDMS samples were cooled down to the room temperature, and during the process an equi-biaxial compression is induced to the a-Si layer due to a large difference in the thermal expansion coefficient between the a-Si layer ($\sim 1\times10^{-6}\,K^{-1}$) and the PDMS ($\sim 3.1\times10^{-4}\,K^{-1}$) [22]. The release of the pre-strain leads to the generation of various patterns on the surface of a-Si film.

The mechanism of the pattern formation and transition during the exertion of equi-biaxial compression to the film was investigated using an *in-situ* optical microscope. The wavelength, defined as the distance between two adjacent peaks, was measured using an image processing software, Image J on Windows operating system. The amplitudes were quantified by XE-100 atomic for microscopy (AFM) of Park System in which the scans of several $100\times100\,\mu m^2$ area are obtained from each sample, along with the use of large surface, high magnification, non-contact white light interferometer of the Zygo's New View 6300 System. The accurate thickness of a-Si film was determined using HITACHI S-4300 field emission scanning electron microscope (FE-SEM) by taking a cross-sectional SEM image on a cleavage of the sample.

3. Results and discussion

Fig. 1(a) schematically illustrates the experimental procedures, and (b)–(d) show the representative optical microscopic images of buckling patterns obtained through the described procedure (heated at 150 °C) according to different locations of the a-Si film: (b) edge, (c) center region, and (d) inner region. The deformed structures exhibited different behaviors according to the positions of their generations as follows: one-dimensional wavy patterns were created near the edges of the sample; disordered two-dimensional structures were observed at center regions; and well ordered two dimensional

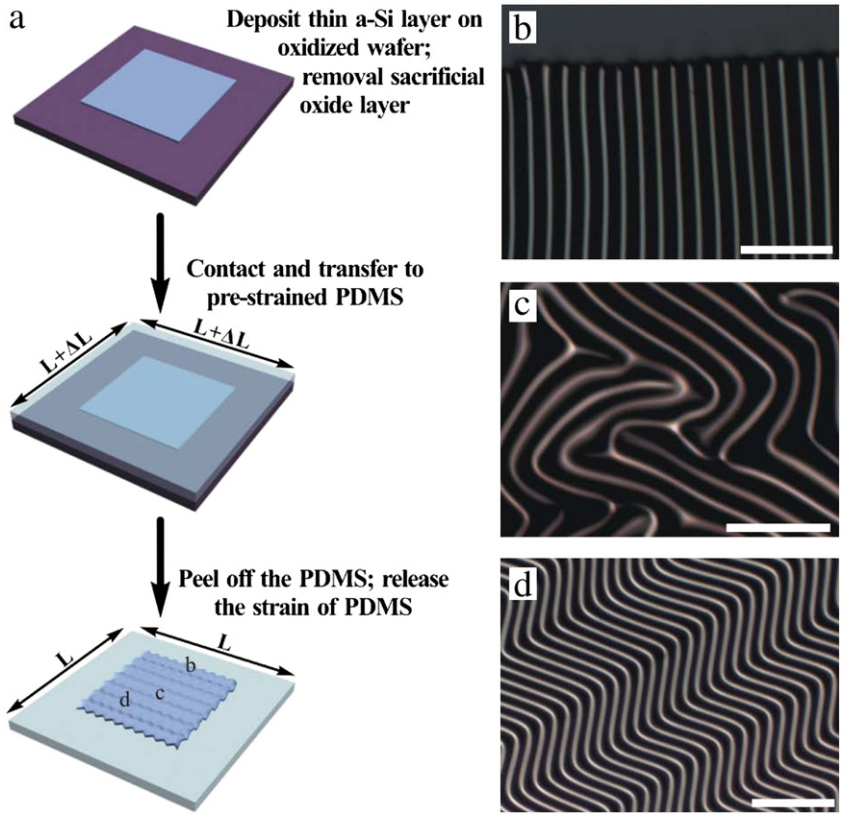

Fig. 1. (a) Schematic illustration of process for obtaining various patterns on a-Si surface. Optical images of the buckled a-Si layer: (b) one-dimensional wrinkles, (c) two-dimensional random ordering, and (d) two-dimensional highly ordered herringbone patterns. The PDMS substrate is thermally pre-strained to 3.8% at 150 °C. The scale bars in the images indicate 100 μm.

wavy patterns, called 'herringbone' structures, were produced far from the edges. The primary cause for the development of wrinkles having various patterns according to different positions can be attributed to the distribution of stress on a compliant substrate. Due to the traction-free edge of the film, a uniaxial stress parallel to the edge is exerted near the edge. However, the stress exertion becomes biaxial towards the central position of the film, mainly because of the merging of free edge effects [23]. The herringbone structure is evolved as a consequence of sequential exertion of the biaxial stress at the inner regions of the film, apart from the edges, and a random ordering pattern is evolved at the central region due to the spontaneous exertion of the stress. The presented observation on texture formation of a-Si layers are in good agreement with the previous findings of Lin et al. [24], where qualitative explanation on the mechanism of two-dimensional buckling formation is reported. It is stated that the different types of texture formation can be controlled by varying the magnitude of the applied mechanical forces and the timings.

To better understand the underlying mechanism of how different types of the patterns are formed according to their positions on the a-Si film as a function of time *t*, an *in-situ* study with optical microscope was conducted while releasing the thermal pre-strain of the a-Si/PDMS samples by natural cooling at room temperature. Fig. 2 illustrates the formation of herringbone structure of the a-Si film, due to an applied perpendicular sequential compressive stress, during the increase of *t*. The PDMS used for this experiment was pre-strained to approximately 3.8% at 150 °C [23], and the thickness of the a-Si film used was 270 nm. The formation of herringbone structure on the surface of the a-Si film is attributed to two different directional, but sequential exertion of a compressive strain, herein after referred as X or Y directional. During the initial stages of the pre-strain release (until 58 s, represented in

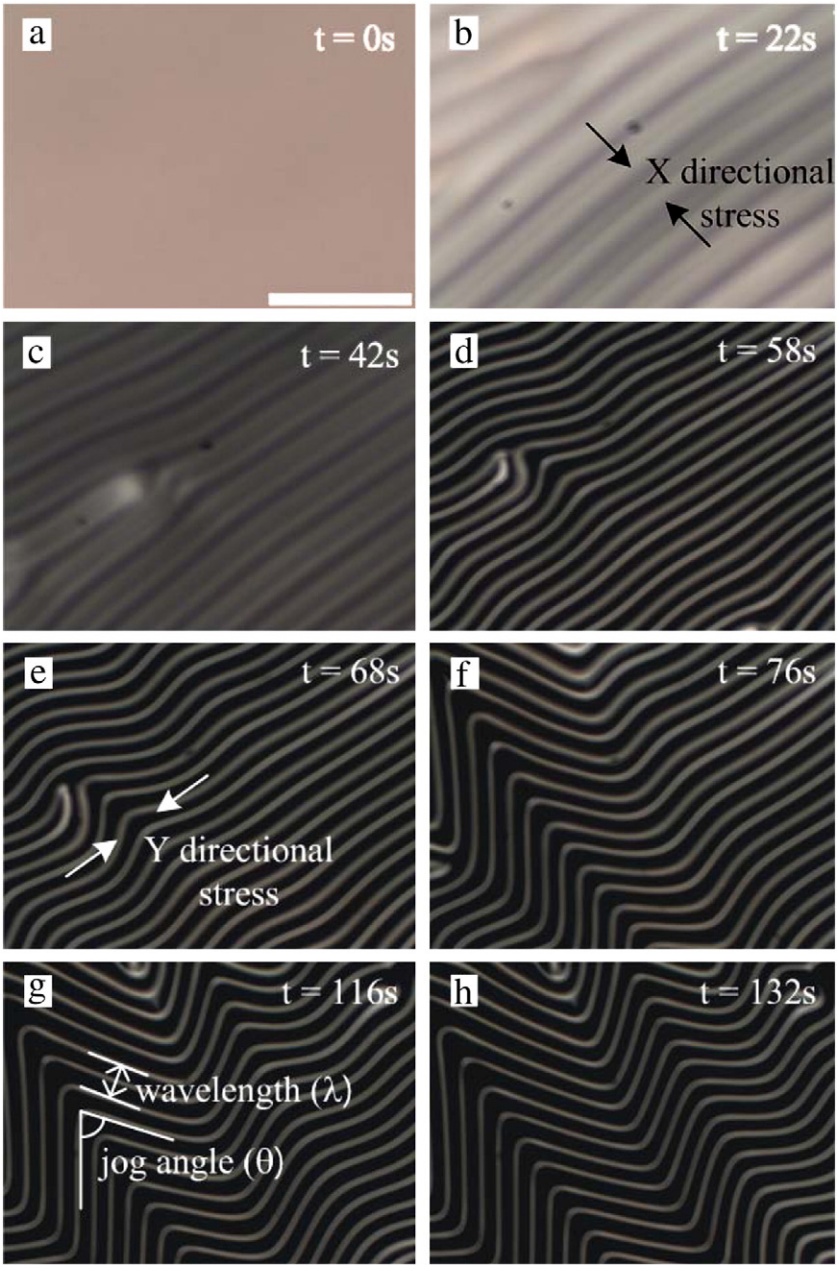

Fig. 2. Optical micrographs showing the formation of herringbone structured patterns as time *t* increases. The X and Y directions of the sequential compressive stresses are depicted in (b) and (e), respectively. The characteristic parameters of the herringbone structure, which are the wavelength and jog angle, are represented in (g). The pre-strain induced in the PDMS substrate was approximately 3.8%. The scale bars in the images indicate 100 μm.

Fig. 2(b)–(d)), one-dimensional wrinkles are predominantly generated on the a-Si film surface owing to an initial force of which the direction is indicated as X, as depicted with an arrow in Fig. 2(b). The well ordered herringbone structure is obtained through further bending by a differently followed compressive strain, of which the direction is perpendicular (depicted as Y in Fig. 2(e)) to the former compressive strain in Fig. 2(b). Hence, it can be concluded that when contraction forces of different directions are applied to the film in a sequential order, a highly ordered herringbone structure is formed; on the other hand, if equi-biaxial strain is exerted to the film simultaneously, a randomly ordered sequence of buckling is formed on the film. The evidence to the aforementioned inference can be found in the previous reports where similar three types of pattern evolutions shown in the case of a-Si thin film were also shown in the films of other materials such as gold and c-Si [12,20,25].

Fig. 3 shows the changes of the jog angle (θ) and wavelength (λ) as a function of *t* obtained from an *in-situ* observation using a 270-nm-thick a-Si sample. The parameters θ and λ refer to the angle of constitutional peaks and the distance between the adjacent peaks, respectively. The aforementioned parameters play a crucial role in determining the characteristics of the herringbone structure along with the amplitude (*A*) of the wavy structures [26,27]. Each parameter is depicted in Fig. 2(g) except for the amplitude. At the very early stage of surface deformation the film develops one-dimensional wrinkles, of which the wavelength is measured to be approximately 38.1 μm with a jog angle of 180° (after 20 s). During the stages shown in the Fig. 2(c)–(e), the pre-strain induces a force in X direction, causing the film to be deformed and λ is decreased from 38.1 μm to 34.8 μm. Two-dimensional buckling, or herringbone structure is completely formed by the introduction of following sequential stress in Y direction (described in Fig. 2(e)–(f)), and after 76 s, λ no longer experiences a further variation and is nearly settled to 32.0 μm. During the time interval of 60 to 80 s, the amount of θ decreases radically to the specific value of 82.8°, and no further significant shifts are found afterwards, similar to the case of the decrease in λ. Despite the fact that temperature and strain have linear relationship with time *t*, a sudden formation of wrinkles was observed during the aforementioned time interval. Presumably, before 60 s, built-up strain by thermal contraction is lower than its critical limit, and thus the film can tolerate the stress without much deformation. Once the amount of applied strain reaches to its critical strain, radical deformations are engendered and herringbone structure is fully developed, causing the dramatic decrease in both λ and θ until 80 s. The in-situ optical microscope observation during the full courses of development of highly ordered zigzag patterns (herringbone structures) shown in Fig. 2 is consistent with the time-based variation results of both λ and θ.

Despite the isotropic manner of the expansion or contraction in the PDMS, the attached a-Si film experiences different directional stresses according to its position, and this can be explained by the fact that the stress in planar X–Y directions has asymmetric distribution according to the location [28]. One-dimensional wrinkles are generated due to a single directional exertion of the force induced by the pre-strain, and two-dimensional random orderings are aroused by simultaneously exerted equi-biaxial forces. The dominant structures formed on the buckled surface are the formation of herringbone shapes rather than the other two modes since the herringbone structure effectively reduces the stresses caused to the surface, having a minimum surface energy compared to the other two structures. In fact, the herringbone structures were found throughout the inner regions of the a-Si film surface, which is in good agreement with the morphology of buckled single crystal Si films obtained in previous reports [17,20].

Fig. 4(a) presents the typical $100 \times 100\ \mu m^2$ AFM image of the herringbone structure in a-Si film obtained through the exertion of isotropic compressive stress at 105 °C. The herringbone patterns obtained on the surface of the a-Si film are characterized by zigzag structures induced by two distinct directional strains, although the compressive strain is completely isotropic in the PDMS. Cross sectional profiles for the samples pre-strained at 105 °C and 150 °C along the dashed line is revealed in Fig. 4(b) and (c), respectively. It is observed that the images and profiles of the buckled herringbone structure are shaped as sinusoidal figures, whose characteristics can be explicitly described by λ and *A* of the wavy structures. For the case of the sample pre-strained at $T_s = 105$ °C, measured values of λ and *A* are 30.8, and 2.7 μm respectively, and for the case of pre-strained sample at 150 °C, λ and *A* are 30.7, and 2.9 μm, respectively. For a larger pre-strain, the wrinkle has a higher *A* than that of smaller pre-strained sample while λ is almost sustained, which is in accordance with the findings of Ref 27. It is reported that λ does not depend on

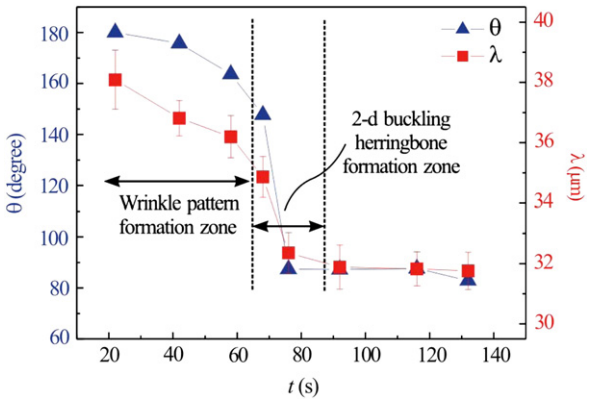

Fig. 3. The change in the aspect of jog angle (left axis) and wavelength (right axis) as a function of *t* during the course of herringbone structure formation.

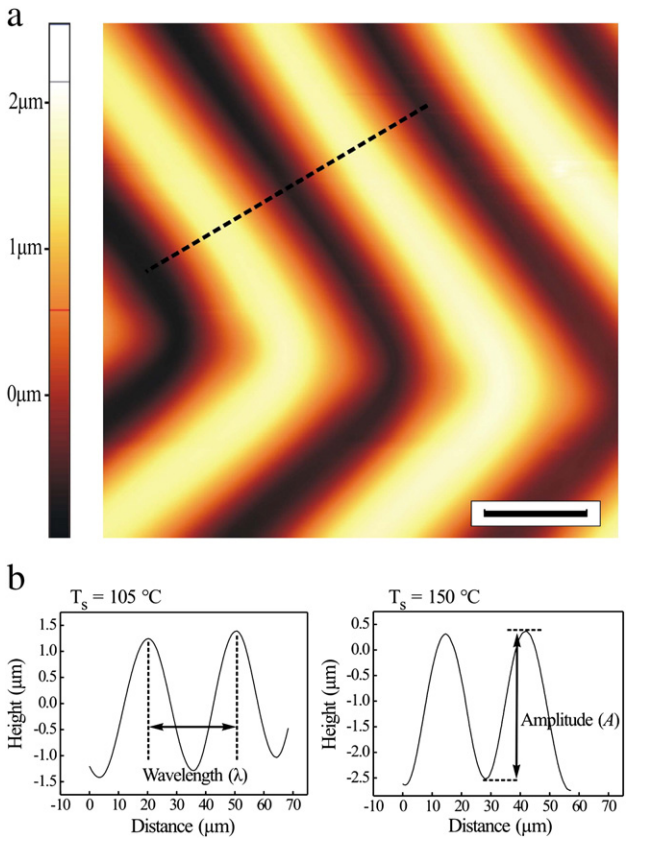

Fig. 4. (a) The AFM image of the two-dimensional herringbone structure on a-Si surface of the sample with $T_s = 105$ °C and (b) the surface profiles of the samples with different pre-strains by applying the annealing temperature of 105 °C and 150 °C.

the amount of pre-strain applied to the system, but rather the mechanical properties such as elastic modulus and thickness of the film play a major role in the determining of λ. On the contrary, *A* is highly affected by the amount of pre-strained exerted to the system, and this relationship is clearly illustrated in the presented results. Hence, the geometry of self-assembled wrinkles can be effectively estimated and its structures and dimension can be controllably manipulated through varying the amount of stress and thickness of the film.

In order to quantitatively investigate the influence of thermally produced pre-strain on the structure parameters, especially λ and *A*, different amounts of pre-strain were released by varying the annealing temperature of the a-Si/PDMS systems from 105 to 150 °C. Fig. 5 plots the corresponding results of increasing *A* in all three patterns with increasing amount of pre-strain in the PDMS substrate. The amount of pre-strain can be calculated using the following equation: $\varepsilon_{\text{pre-strain}} = \Delta\alpha \times \Delta T$ [20], where $\Delta\alpha$ is the difference in the thermal expansion coefficients of PDMS and a-Si film whose values are $\alpha_{\text{PDMS}} = 3.1 \times 10^{-4} K^{-1}$ and $\alpha_{\text{a-Si}} = 1 \times 10^{-6} K^{-1}$. Based upon the above equation, the amounts of induced pre-strain in the PDMS were estimated to be approximately 2.47, 2.94, 3.40, and 3.86 % for the corresponding temperatures of 105, 120, 135, and 150 °C, respectively. A linear relationship between the amount of pre-strain and *A* were observed for the one and two-dimensional patterns, whose values increased from 2.1 to 2.7 μm for the one-dimensional structures and 3.1 to 4.1 μm for the two-dimensional structures with increasing the amount of pre-strain.

To conduct a comparative analysis of the obtained experimental results and theoretically estimated values of *A*, the estimated *A* of the one-dimensional patterns on a-Si film can be calculated using the following equation which was derived using the energy minimization method [17]:

$$A_{1d} = h_f \cdot \sqrt{\frac{\varepsilon_{pre}}{\varepsilon_{1d}^c} - 1} \tag{1}$$

where ε_{1D}^c is the critical strain for the one-dimensional buckling mode,

$$\varepsilon_{1d}^c = \left(3\overline{E_s}/3\overline{E_f}\right)^{2/3} / 4(1 + \nu_f). \tag{2}$$

h_f is the thickness of the a-Si film, and ε_{pre} is the induced pre-strain. For Eq. (2), $\overline{E_f}$ and $\overline{E_s}$ are the plane-strain modulus of film and substrate, respectively, whose values may be calculated using the Poisson's ratio of film ν as follows: $\overline{E_{f,s}} = E_{f,s} / \left(1 - \upsilon_{f,s}^2\right)$. For the calculation of *A*, literature values were used: $E_{\text{PDMS}} = 1.8$ Mpa, $\nu_{\text{PDMS}} = 0.48$, $E_{\text{a-si}} = 80 \pm 20$ Gpa, and $\nu_{\text{a-si}} = 0.22$ [29,30]. The calculated values of A_{1d} were 2.1, 2.3, 2.5, and 2.7 μm and the corresponding amount of applied pre-strains were 2.47%, 2.94%, 3.40%, and 3.86%, respectively (plotted as dash-dotted line in Fig. 5).[1] Considering the amount of uncertainties in experiments, the experimental observations are in perfect match with the calculated values. While the accurate analytical solutions on the development of one-dimensional buckling mode is well established, the analytical modeling of two-dimensional random ordering on compliant substrate can only be described by a set of complex nonlinear partial differential equations. Thus, we applied the analytical solutions of the checkerboard to the following 2D random patterns' analyses, since the mechanism of 2D random ordering pattern formation is identical with that of checkerboard patterns except for the amount of pre-strain applied on the membrane [25]. The checkerboard patterns are developed when the magnitude of simultaneously equi-biaxial strain is slightly larger than the critical strain, while the 2D random ordering patterns are formed by much larger amounts of strain. In this approximation, similar aspects can be found for the two-dimensional wavy patterns, where the theoretical values of *A* can be obtained from the following equation [17]:

$$A_{2d} = h_f \cdot \sqrt{\frac{8}{(3-\nu_f)(1+\nu_f)}\left(\frac{\varepsilon_{pre}}{\varepsilon_{2d}^c} - 1\right)} \tag{3}$$

where ε_{2d}^c is the critical strain for the two dimensional buckling mode,

$$\varepsilon_{2d}^c = \left(3\overline{E_s}/\overline{E_f}\right)^{2/3} / 4(1 + \nu_f). \tag{4}$$

Here, the values of *A* are matched well with respect to the experimental results (3.3, 3.6, 3.8, and 4.1 μm, in the order of increasing the annealing temperature) and the corresponding data are plotted as dashed line in Fig. 5.[1] Hence, it can be concluded that the analytical equations used to determine the development of checkerboard patterns can be expanded to describing the evolution of 2D random ordering structures. Comparative analysis for the parameters of the herringbone structure was not performed since the theoretical estimations cannot be obtained in the form of analytical equations [17]. However, we were able to observe a similar tendency where the values of *A* linearly increased as a function of the pre-strain; therefore, it can be generally inferred that the *A* of various patterns on a-Si film can be adjustable by controlling the amount of pre-strain.

To solidify the validity of the measured values of λ in the different buckling modes with respect to theoretical approaches, the following equations were used for the calculation of λ in one and two-dimensional modes, respectively [27]:

$$\lambda_{1d} = h_f \cdot \left(\frac{\overline{E_f}}{3\overline{E_s}}\right)^{1/3}. \tag{5}$$

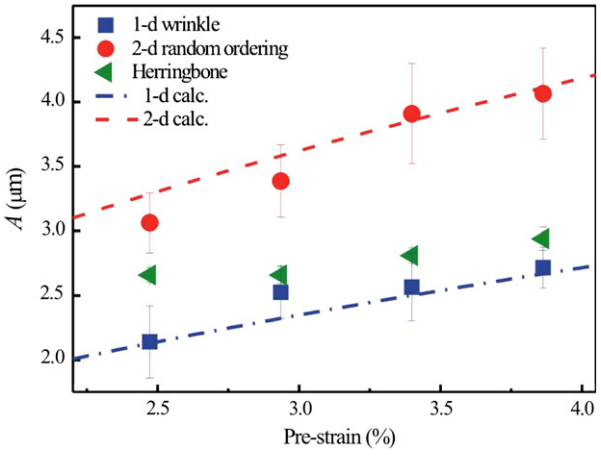

Fig. 5. The changes of amplitude as a function of pre-strain for the various patterns generated on the surface of a-Si film. The dash-dotted line and dashed line represent the theoretically estimated values of the amplitudes for one-dimensional and two-dimensional random ordering mode, respectively.

[1] The plotted line in Fig. 5 for the amplitudes of one-dimensional wrinkled patterns and two-dimensional wavy structures were characterized by the following equations:

$$A_{1d} = 2.7 \times 10^{-7} \times \sqrt{\frac{x}{3.91 \times 10^{-4}} - 1},$$

$$A_{2d} = 2.7 \times 10^{-7} \times \sqrt{\frac{2.36 \times x}{3.91 \times 10^{-4}} - 1},$$

where *x* is the amount of pre-strain and A_{1d}, A_{2d} are the amplitudes of one-dimensional wrinkled patterns and two-dimensional wavy structures, respectively.

$$\lambda_{2d} = \sqrt{2}\cdot h_f \cdot \left(\frac{\bar{E}_f}{3\bar{E}_s}\right)^{1/3}. \quad (6)$$

The wavelength of one-dimensional wrinkle is estimated to be 38.8 μm, which is in consistency with the experimental result of 39.0 μm within experimental uncertainties. However, for the two dimensional structure, where the patterns are formed by spontaneous equi-biaxial stress, a slight discrepancy was found in between the experimental results and theoretical measurements (50.3 μm and 54.9 μm, respectively). Such inconsistency in the values of λ can be ascribed to the fact that the equation of wavelength for checkerboard is not in perfectly well matched with the case of random ordering patterns and thus, a larger amount of uncertainties has to be taken into consideration. All these results indicate that the amplitude of wrinkled patterns increases as the pre-strain increases, while the wavelength does not depend on the induced force. Note that the invariance of λ as a function of pre-strain in our experimental ranges is in good agreement with the findings of Jiang et al. [31] which explains that wavelength would not change for the applied pre-strain below ~10%. Hence, it can be inferred that it is possible to control the aspect ratio between the wavelength and amplitude to acquire specific dimensions of deformed a-Si films.

4. Conclusion

We performed the formation of buckled structure on a-Si layer through thermally induced biaxial strain in PDMS and carefully observed the evolution of surface deformation using an *in-situ* optical microscope. The various sinusoidal wrinkled patterns were generated with distinct geometries which are affected by the following parameters: the positions of their generation, the thickness of a-Si layer, the level of induced pre-strain, and mechanical property of film. The theoretical solutions, which were established in previous researches for the c-Si membrane, were applied to a-Si layer, and the estimated values were in good accordance with our experimental results. These consistencies indicate that the deformation modeling of c-Si film can be expandable to that of a-Si membrane. The magnitude of thermally induced pre-strain has a linear relationship with the increase in the amplitude of the wavy structures; on the other hand, the wavelengths of the wavy structures are independent of the amount of pre-strain of 3.86%. Thus, the understanding on the mechanism of buckled structure formation on a-Si surfaces exploited in this article will facilitate the controllability of dimensions for textured a-Si thin films as well as c-Si films.

Acknowledgements

This work was partly supported by the IT R&D program of MKE/KEIT [10030517-2009-03, Advanced CMOS image sensor using 3D integration] and by Priority Research Centers Program through the National Research Foundation of Korea (NRF) funded by the Ministry of Education, Science and Technology [2009-0093823].

References

[1] C.W. Han, M.K. Han, S.H. Paek, C.D. Kim, I.J. Chung, Electrochem. Solid-State Lett. 10 (2007) J65.
[2] Theiss, S. Wagner, IEEE Electron. Dev. Lett. 17 (1996) 578.
[3] C.C. Striemer, T.R. Gaborski, J.L. McGrath, P.M. Fauchet, Nature 445 (2007) 749.
[4] V. Baranchugov, E. Markevich, E. Pollak, G. Salitra, D. Aurbach, Electrochem. Commun. 9 (2007) 796.
[5] T. Moon, C. Kim, B. Park, J. Power Sources 155 (2006) 391.
[6] R.A. Street, R.L. Weisfield, R.B. Apte, S.E. Ready, A. Moore, M. Nguyen, W.B. Jackson, P. Nylen, Thin Solid Films 296 (1997) 172.
[7] A. Shah, P. Torres, R. Tscharner, N. Wyrsch, H. Keppner, Science 285 (1999) 692.
[8] R.P. Nair, M. Zou, Surf. Coat. Technol. 203 (2008) 675.
[9] J. Wienke, B. van der Zanden, M. Tijssen, M. Zeman, Sol. Energy Mater. Sol. Cells 92 (2008) 884.
[10] J. Müller, O. Kluth, S. Wieder, H. Siekmann, G. Schöpe, W. Reetz, O. Vetterl, D. Lundszien, A. Lambertz, F. Finger, B. Rech, H. Wagner, Sol. Energy Mater. Sol. Cells 66 (2001) 275.
[11] N. Bowden, S. Brittain, A.G. Evans, J.W. Hutchinson, G.M. Whitesides, Nature 393 (1998) 146.
[12] X. Chen, J.W. Hutchison, Scr. Mater. 50 (2004) 797.
[13] H. Fei, H. Jiang, D.Y. Khang, J. Vac. Sci. Technol. A 27 (2009) L9.
[14] D.Y. Khang, H. Jiang, Y. Huang, J.A. Rogers, Science 311 (2006) 208.
[15] N. Bowden, W.T.S. Huck, K.E. Paul, G.M. Whitesides, Appl. Phys. Lett. 75 (1999) 2557.
[16] C.M. Stafford, B.D. Vogt, C. Harrison, D. Julthongpiput, R. Huang, Macromolecules 39 (2006) 5095.
[17] J. Song, H. Jiang, W.M. Choi, D.Y. Khang, Y. Huang, J.A. Rogers, J. Appl. Phys. 103 (2008) 014303.
[18] K. Lee, S. Lee, D.Y. Khang, T.Y. Lee, Soft Matter 6 (2010) 3249.
[19] Y.G. Sun, W.M. Choi, H. Jiang, Y.Y. Huang, J.A. Rogers, Nature 1 (2006) 201.
[20] P.C. Lin, S. Yang, Appl. Phys. Lett. 90 (2007) 241903.
[21] E.A. Wilder, S. Guo, S. Lin-Gibson, M.J. Fasolka, C.M. Stafford, Macromolecules 39 (2006) 4138.
[22] K. Takimoto, A. Fukuta, Y. Yamamoto, N. Yoshida, T. Itoh, S. Nonomura, J. Non-Cryst. Solids 299–302 (2002) 314.
[23] W.M. Choi, J. Song, D.Y. Khang, H. Jiang, Y.Y. Juang, John A. Rogers, Nano Lett. 7 (2007) 1655.
[24] P.C. Lin, S. Yang, Appl. Phys. Lett. 90 (2007) 241903.
[25] Z.Y. Huang, W. Hong, Z. Suo, J. Mech. Phys. Solids 53 (2005) 2101.
[26] X. Chen, J.W. Hutchinson, J. Appl. Mech. 71 (2004) 597.
[27] J. Song, H. Jiang, Y. Huang, J.A. Rogers, J. Vac. Sci. Technol., A 27 (2009) 1107.
[28] D. Khang, J. Rogers, H. Lee, Adv. Funct. Mater. 19 (2009) 1526.
[29] A. Bietsce, B. Michel, J. Appl. Phys. 88 (2000) 4310.
[30] L.B. Freund, S. Suresh, Thin film materials, Cambridge University Press, Cambridge, 2003, p. 96.
[31] H. Jiang, D. Khang, J. Song, Y. Sun, Y. Huang, J. Rogers, Proc. Nat. Acad. Sci. 104 (2007) 15607.